Journal of Nuclear Materials 393 (2009) 153–161

Contents lists available at ScienceDirect

Journal of Nuclear Materials

journal homepage: www.elsevier.com/locate/jnucmat

Cluster Dynamics modelling of irradiation growth of zirconium single crystals

F. Christien [a,*], A. Barbu [b]

[a] Université de Nantes, Polytech'Nantes, LGMPA, Rue Christian Pauc, BP 50609, F-44306 Nantes cedex 3, France
[b] Service de Recherches de Métallurgie Physique, CEA Saclay, 91191 Gif-sur-Yvette, cedex, France

ARTICLE INFO

Article history:
Received 11 February 2009
Accepted 28 May 2009

PACS:
61.72.J
61.80.Hg
61.82.Bg

ABSTRACT

This paper aims at modelling irradiation growth of zirconium single crystals as a function of neutron fluence. The Cluster Dynamics approach is used, which makes it possible to describe the variation of irradiation microstructure (dislocation loops) with neutron fluence. From the irradiation microstructure, the strain can be calculated along the axes of the lattice structure. The model is applied to the growth of annealed zirconium single crystals at 553 K measured by Carpenter and Rogerson in 1981 and 1987. The model is found to fit the experimentally measured growth of Zr single crystals very nicely, even at large neutron fluence where the 'breakaway growth' occurs. This was made possible by considering in the model the growth of vacancy loops in the basal planes. This growth of vacancy loops in the basal planes could be modelled by taking into account that diffusion of self-interstitial atoms (SIA) is anisotropic and that there exist in the basal planes some nucleation sites for vacancy loops (iron clusters), the density of which is considered constant over time.

1. Introduction

It is well known that zirconium alloys submitted to neutron irradiation are subject to 'irradiation growth', that-is-to-say an anisotropic strain without any external stress. From the experimental point of view, irradiation growth of zirconium alloys was extensively studied in the past (see for example [1]): effect of grain size, alloying elements, cold working... Many models based on different mechanisms for irradiation growth have already been proposed in the literature [2–8]. Nevertheless, modelling of zirconium irradiation growth is still of interest for several reasons:

1. *First, the existing models mentioned above do not really describe the evolution of the dislocation loop microstructure (in terms of loop density and loop mean radius) during irradiation.* This should however be taken into account for a complete modelling of irradiation growth. In these models, the dislocation loop density is an input of the calculation and is supposed not to change with time, which is not true, especially at the beginning of irradiation...
2. *Second, some of these models* [2–5] *do not take the DAD (Diffusion Anisotropy Difference) effect:* it has been demonstrated that in zirconium diffusion of self-interstitial atoms (SIA) is anisotropic [9–13] (whereas vacancy diffusion can reasonably be considered isotropic). This Diffusion Anisotropy Difference (DAD) can induce a large bias that can 'completely dominate the conventional dislocation bias caused by first order elastic interaction between the point defects and the sink' (cited from [7]). Moreover it has been shown that the DAD theory can explain some important aspects of zirconium growth [14,15].
3. *Third, many important data (formation and binding energies, diffusion coefficients, diffusion anisotropy...) are now available for zirconium in the literature*, in particular thanks to the recent improvements of simulation techniques (molecular dynamics for example). Although these data have to be considered with caution, they are of great interest for the calculation of zirconium irradiation growth.

In this paper, we will propose a model for zirconium irradiation growth, based on the Cluster Dynamics approach [16,17] that enables to describe the evolution of the dislocation loop microstructure under irradiation for very long times. The DAD effect will be taken into account. We will apply the model to the experimental results published by Rogerson [18] in 1987 (who continued the work by Carpenter et al. [19] in 1980) on growth of Zr single crystals irradiated with neutrons at 553 K. Particular attention will devoted to the 'breakaway growth' effect.

1.1. Description of the experimental results concerning irradiation growth of zirconium single crystals [18,19]

The experimental results exposed here are taken from references [18,19]: cylindrical specimens of annealed pure zirconium (127 mm long and 4.5 mm diameter) were irradiated at 553 K in fast neutrons fluxes of between 5.3 and 7.6×10^{17} nm^{-2} s^{-1} (DIDO reactor). This neutron flux was converted into a point defect production rate using the proportionality factor published in Ref.

* Corresponding author. Tel.: +33 2 40 68 31 72; fax: +33 2 40 68 31 99.
E-mail address: frederic.christien@univ-nantes.fr (F. Christien).

0022-3115/$ - see front matter © 2009 Elsevier B.V. All rights reserved.
doi:10.1016/j.jnucmat.2009.05.016

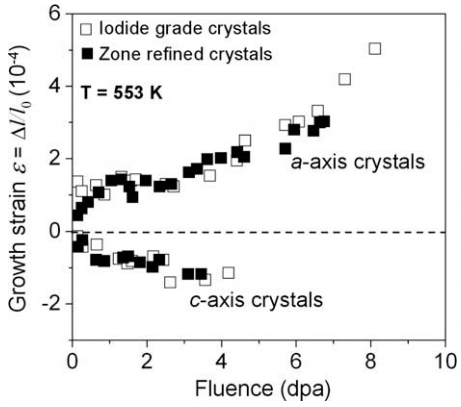

Fig. 1. Irradiation growth of *a*-axis and *c*-axis zirconium single crystals at 553 K. Neutron irradiation (6.5×10^{17} nm^{-2} s^{-1} $\approx 10^{-7}$ dpa s^{-1}). From Rogerson [18] and Carpenter et al. [19].

[20] and calculated using the DISPKAN program developed by Woo [21]. A point defect production rate of $\sim 10^{-7}$ dpa s^{-1} was obtained. Iodide grade (open symbols on Fig. 1) and zone refined (full symbols on Fig. 1) single crystals were used. The '*a*-axis' crystals are oriented so that the angle φ between the main axis of the single crystal and the *c*-axis of the lattice structure is closed to 90° (79° for the iodide grade crystal and 87° for the zone refined crystal). Concerning the '*c*-axis' crystals, the angle φ is 26° for the iodide grade crystal and 28° for the zone refined crystal. The irradiation growth of the *a*-axis and *c*-axis crystals is shown in Fig. 1. It consists of an expansion of the *a*-axis crystals and a contraction of the *c*-axis crystals. A transient growth is first observed on the *a*-axis single crystals, followed by saturation at about 1.2×10^{-4}. Then, above a certain fluence (~2–3 dpa), the expansion of the *a*-axis single crystals starts increasing again ('breakaway growth'). The contraction of the *c*-axis crystals seems to be more monotonous and the 'breakaway' effect is not so obvious.

1.2. Description of the experimental results concerning loop microstructure in irradiated zirconium [22–26]

Dislocation loops that form in zirconium under irradiation (electron or neutron) can be classified into two types according to their Bürgers vector:

- The *prismatic* loops or *a*-loops: they have a $\vec{b} = 1/3$ <1 1 2 0> Bürgers vector (parallel to the *a*-axis of the lattice structure). They are lying approximately in the prismatic planes $(1\,0\,\bar{1}\,0)$. In certain situations, both vacancy and interstitial loops can coexist [17,22–24].
- The *basal* loops or *c*-loops: they are lying in the (0 0 0 1) plane and their Bürgers vector has a component along the *c*-axis. These loops are almost always vacancy type. They can be perfect loops ($\vec{b}$ = <0 0 0 1>) or imperfect loops ($\vec{b} = 1/2$ <0 0 0 1> or $\vec{b} = 1/6$ $<2\,0\,\bar{2}\,3>$).

During neutron irradiation, *a*-loops form first. *c*-Loops formation is observed only above a certain fluence that depends on solute concentrations and temperature [22,26]. It has been shown that the 'breakaway growth' of zirconium alloys under neutron irradiation correlates with the appearance of vacancy *c*-loops that act as vacancy sinks [26,27].

1.3. The Cluster Dynamics Model

A model based on the Cluster Dynamics approach was proposed in [16] that describes the evolution of the dislocation loop microstructure under irradiation. It calculates the variation with time of the size distribution of the dislocation loop population. This model cannot be directly applied to α-zirconium since it is based on the assumption that point defect diffusion is isotropic, which is not true for zirconium. In Ref. [17], this Cluster Dynamics Model was then extended to the case where the diffusion of self-interstitial atoms (SIA) is anisotropic, as in zirconium (for a detailed description of this 'extended' Cluster Dynamics Model, see Ref. [17]). In that 'extended' model, only SIA diffusion is assumed to be anisotropic, whereas vacancy diffusion is supposed isotropic [9–13]. It should be emphasized that in this model, only point defects are supposed mobile. On the contrary, point defect clusters are assumed immobile.

1.3.1. Point defect sinks

All types of point defect sinks existing in zirconium single crystals can be taken into account in the 'extended' model (surfaces, dislocation lines existing before irradiation, and dislocation loops):

1. *Surfaces:* in fact, since the single crystals are large, it can be checked that the effect of surfaces on point defect absorption and emission is absolutely negligible.
2. *Dislocation lines:* the single crystals are annealed so that the dislocation density before irradiation is supposed to be small. The dislocation density will be taken equal to 10^6 cm^{-2} and it will be assumed that these dislocation lines are parallel to the *c*-axis with a Bürgers vector $\vec{b} = 1/3$ <1 1 2 0>. Anyway, it was checked that this dislocation density can vary from 0 to 10^8 cm^{-2} without any strong effect on the calculation.
3. *Dislocations loops:* dislocations loops are the main point defect sinks. In a first step, only prismatic loops (*a*-loops) will be considered. They are supposed to lie in the prismatic $(1\,0\,\bar{1}\,0)$ planes and to have a $\vec{b} = 1/3$ <1 1 2 0> Bürgers vector. Basal loops (*c*-loops) will be introduced in the model in a second step in order to model the 'breakaway growth'.

One of the main points of the 'extended' model is that Z_i^a the efficiency factor relative to the absorption of SIA by prismatic dislocation loops (*a*-loops) is a function of the SIA diffusion anisotropy [17]:

$$Z_i^a = z_i \times \frac{1}{3}\left(p + \frac{\sqrt{3+p^6}}{p^2}\right), \tag{1}$$

where z_i is a term describing the SIA/dislocation elastic interaction ($z_i = 1.1$ [15,34]) and p is the SIA diffusion anisotropy factor defined by [15]:

$$p = \left(\frac{D_i^c}{D_i^a}\right)^{1/6}. \tag{2}$$

D_i^a is the SIA diffusion coefficient along the *a*-axis of the lattice structure and D_i^c is the SIA diffusion coefficient along the *c*-axis. It has been shown that $D_i^a > D_i^c$ [9–13], so that $p < 1$ and $Z_i^a > z_i$. Thus, the SIA diffusion anisotropy leads to a better SIA absorption efficiency by prismatic loops.

1.3.2. Points defect creation

Due to the lack of data available in the literature concerning point defect cluster formation within cascades under neutron irradiation in zirconium, it was assumed here that point defect were created here as Frenkel pairs (isolated vacancies and SIA) at a rate of 10^{-7} dpa s^{-1}.

In the following, we will show how the 'extended' Cluster Dynamics Model can be used to calculate irradiation growth of zirconium. As mentioned before, we will focus here on zirconium

single crystals and will compare the calculations to the experimental data presented above (Fig. 1).

2. Cluster Dynamics modelling of zirconium single crystal growth before 'breakaway growth'

2.1. Calculation of the strains along the a-axis, c-axis and crystal axis

We focus here on dimensional changes due to prismatic dislocation loop formation during irradiation. In a first step, we consider the growth of zirconium single crystals before 'breakaway growth' occurs. That is why, in this first step, the only loops that have to be considered are prismatic loops since basal loops form only above a certain fluence (~2–3 dpa) corresponding to the occurrence of 'breakaway growth' [22,26].

From the size distribution of prismatic dislocation loops calculated by the Cluster Dynamics Model, it is possible to calculate the relative strain ε_a along the a-axis [2]:

$$\varepsilon_a = \frac{1}{2} Q_i^a V_{at}, \tag{3}$$

where Q_i^a is the net quantity of SIA in the a-loops expressed per unit volume and V_{at} is the atomic volume. Q_i^a is given by:

$$Q_i^a = Q_i^{ia} - Q_v^{va}, \tag{4}$$

where Q_i^{ia} is the number of SIA in the *i*nterstitial a-loops (ia) and Q_v^{va} is the number of vacancies in the *v*acancy a-loops (va). Q_i^{ia} and Q_v^{va} are also expressed per unit volume.

If it is assumed that the number of vacancies and SIA created by irradiation is the same, the assessment of the number of created, recombined and eliminated point defects (on dislocation lines, dislocation loops and surfaces) leads to:

$$Q_i^{ia} = C_{1v} - C_{1i} - Q_i^s - Q_i^d, \tag{5}$$

where C_{1v} is the number of vacancies per unit volume, C_{1i} is the number of SIA per unit volume, Q_i^s is the net quantity of SIA (SIA minus vacancies) that has eliminated on surfaces and Q_i^d is the net quantity of SIA that has eliminated on pre-existing dislocation lines. It should be noticed that in the particular case of large single crystals with a low density of pre-existing dislocations lines, the terms Q_i^s and Q_i^d could be neglected, except at the very beginning of irradiation.

Then, from Eqs. (3) and (5), it is possible at every moment during the Cluster Dynamics calculation to calculate the strain along the a-axis associated with the formation of prismatic loops.

It should be emphasized that the net quantity of SIA in the a-loops Q_i^a, as calculated from Eq. (5), includes all the prismatic clusters, even those containing only two point defects. In others words, all the prismatic clusters containing two or more point defects are considered as dislocation loops taking part in the strain along the a-axis. It should be noticed nevertheless that the dominating contribution to the strain along the a-axis is the one of the large interstitial a-loops (see Fig. 4). In other words, including or not the very small prismatic clusters in the calculation of the strain along the a-axis have negligible effect on the result.

We will now focus on the calculation of the strain along the c-axis. Point defect absorption on the prismatic loops induces no strain along the c-axis since the prismatic loops have a $\vec{b} = 1/3 <1\,1\,2\,0>$ Bürgers vector parallel to the a-axis. Nevertheless, it is obvious from Fig. 1 that there is a contraction along the c-axis. This strain, in the first moments of irradiation (<1 dpa), is not likely to be associated with the formation of vacancy basal loops since vacancy basal loops form only above a certain irradiation fluence. It will be assumed that the strain along the c-axis in the first moments of irradiation is due to vacancy relaxation. Vacancy relaxation volume will be taken equal to 0.43 following the ab initio calculations made by Le Bacq and Willaime [28]. Furthermore, it will be assumed that vacancy relaxation is anisotropic and is fully oriented along the c-axis as suggested in [29,30]. The effect of SIA relaxation on the strain will not be taken into account here since the SIA concentration is negligible (see Fig. 5).

The relative strain ε_c along the c-axis is then given by [2]:

$$\varepsilon_c = -C_{1v} V_v^{rel} V_{at}, \tag{6}$$

where C_{1v} is the number of vacancies per unit volume, V_v^{rel} is the vacancy relaxation volume and V_{at} is the atomic volume.

In order to compare the calculated strain with the experimental results of Fig. 1, one has first to calculate the growth strain ε_g along the main axis of the single crystal:

$$\varepsilon_g = \varepsilon_a \sin^2 \varphi + \varepsilon_c \cos^2 \varphi, \tag{7}$$

where φ is the angle between the main axis of the single crystal and the c crystallographic axis. φ is equal to 83° on average for the a-axis crystals (φ = 79° the iodide grade crystal and φ = 87° for the zone refined crystal) and equal to 27° on average for the c-axis crystals (26° for the iodide grade crystal and 28° for the zone refined crystal).

The main features and assumptions of the Cluster Dynamics Model used in this work are summarized in Appendix.

Table 1
Inputs introduced in the Cluster Dynamics Model to describe irradiation growth of Zr single crystals. These inputs are needed by the Cluster Dynamics Model to calculate the variation with time of the size distribution of interstitial and vacancy loops.

			Reference/ comment
Temperature	T	553 K	[18,19]
Point defect creation rate	G	10^{-7} dpa s^{-1}	[18,19,20]
Vacancy formation energy	E_v^f	1.79 eV	[31]
SIA formation energy	E_i^f	3.77 eV	[31]
Di-vacancy binding energy[a]	E_{2v}^B	0.22 eV	[32]
Di-interstitial binding energy[a]	E_{2i}^B	1.42 eV	[17]
Vacancy diffusion coefficient at 553 K	D_v	3.0×10^{-17} $cm^2.s^{-1}$	Adjusted input
SIA diffusion coefficient at 553 K[b]	$\overline{D}_i$	10^{-6} cm^2 s^{-1}	Adjusted input
SIA diffusion anisotropy factor at 553 K	p	0.765	[11–13]
Recombination radius	r_{iv}	10^{-7} cm	[33]
Vacancy/dislocation elastic interaction	z_v	1.0	
SIA/dislocation elastic interaction	z_i	1.1	[15,34]
Bürgers vector (prismatic loops)	b	3.23×10^{-8} cm	[22]

[a] The di-vacancy and di-interstitial binding energy is needed to calculate the binding energy of the loops as a function of their size (see [17] for a detailed explanation).

[b] $\overline{D}_i$ is the SIA mean diffusion coefficient: $\overline{D}_i = (D_i^{a^2} D_i^c)^{1/3}$, where D_i^a is the SIA diffusion coefficient along the a-axis and D_i^c is the SIA diffusion coefficient along the c-axis.

Table 2
Inputs introduced in the Cluster Dynamics Model to describe irradiation growth of Zr single crystals. These inputs are needed to calculate the crystal strain according to Eqs. (3), (6) and (7).

Atomic volume		V_{at}	2.33×10^{-23} cm^3	
Vacancy relaxation volume[a]		V_v^{rel}	0.43	[28]
Single crystal orientation	a-axis crystals	φ	83°	[18,19]
	c-axis crystals		27°	[18,19]

[a] It was assumed in the model that vacancy relaxation is anisotropic and is fully oriented along the c-axis as suggested in [29,30]. Nevertheless, even considering an isotropic vacancy relaxation, it is still possible to get a very good fit of the growth experimental data by re-adjusting the value of V_v^{rel}, $\overline{D}_i$ and D_v to V_v^{rel} = 0.8, $\overline{D}_i = 5.0 \times 10^{-8}$ cm^2 s^{-1} and $D_v = 6.0 \times 10^{-18}$ cm^2 s^{-1}.

2.2. Inputs of the model

We have two different kinds of inputs:

1. First, the inputs needed by the Cluster Dynamics Model to calculate the variation with time of the size distribution of interstitial and vacancy loops are summarized in Table 1.
2. Second, the inputs listed in Table 2, that appear in Eqs. (3), (6) and (7), are those used to calculate the strain.

2.3. Results and discussion

The SIA and vacancy diffusion coefficient $\overline{D}_i$ and D_v were adjusted to get the best fit between the calculated growth curve for *a*-axis crystals and the experimental points taken from [18,19]. The result is shown in Fig. 2. A good agreement is obtained between calculated curves and experimental points. The strain along the real crystallographic *a*-axis and *c*-axis are shown in Fig. 3. The difference observed between strain along the real crystallographic axes and strain along the main axis of the single crystals is due crystallographic orientation of the '*a*-axis' and '*c*-axis' single crystals ($\varphi = 83°$ and 27°, respectively).

Neglecting the absorption of SIA on pre-existing dislocation lines and surfaces and considering that the SIA concentration is much lower than the vacancy concentration (which is always true except in the very beginning of irradiation), we get from Eqs. (3) and (5):

$$\varepsilon_a = \frac{1}{2} C_{1v} V_{at}. \tag{8}$$

Combining Eqs. (6) and (8), we get:

$$\frac{\varepsilon_c}{\varepsilon_a} = -2V_v^{rel} = -0.86. \tag{9}$$

This ratio is consistent with the dotted lines observed on Fig. 3.

We give here an interpretation of the shape of the growth curves plotted on Figs. 2 and 3. If we look at the loop size distribution calculated by the Cluster Dynamics Model for vacancy and interstitial loops, we observe (Fig. 4) that interstitial loops grow whereas vacancy loops do not (only very small vacancy clusters are predicted by the model). This growth of interstitial prismatic loops is the reason of the elongation of the *a*-axis crystals between 0 and 3 dpa (i.e. before breakaway growth), whereas the contraction of the *c*-axis crystals is due to vacancy relaxation along the *c*-axis (as assumed before). At the beginning of irradiation, prismatic dislocation loops absorb much more SIA than vacancies because $\overline{D}_i C_{1i} \gg D_v C_{1v}$ ($C_{1i} \approx C_{1v}$ and $\overline{D}_i \gg D_v$), which corresponds to a fast growth of interstitial loops. Then, vacancy concentration increases until $D_v C_{1v}$ gets close to $\overline{D}_i C_{1i}$. As a consequence, interstitial prismatic dislocation loops absorb more and more vacancies, which makes the growth rate lower and lower. In the permanent regime (above 1 dpa), prismatic dislocation loops absorb so many vacancies as SIA and the crystals do not grow any longer.

As mentioned above, the model predicts the growth of interstitial *a*-loops only and not vacancy *a*-loops. It should be recognized that this is not exactly in agreement with experimental observation of both interstitial and vacancy co-existing *a*-loops in neutron-irradiated zirconium or zirconium alloys (see for example Ref. [22]). Nevertheless, these observations were made on polycrystalline materials (not on single crystals) and it has been demonstrated that anisotropic absorption of point defects on grain boundaries can lead in certain situations to the nucleation and growth of vacancy *a*-loops (see for example the analysis by Woo in Ref. [35]). In the case of the zirconium single crystals used for growth measurements in the original papers by Rogerson and Carpenter we are referring to in this work [18,19], no experimental microstructure analysis was made after irradiation to determine the nature of the *a*-loops. If the prediction of our model is right, the *a*-loops in these single crystals should be of interstitial type.

Let us now come back to the interpretation of the shape of the growth curves plotted on Figs. 2 and 3. As far as the contraction

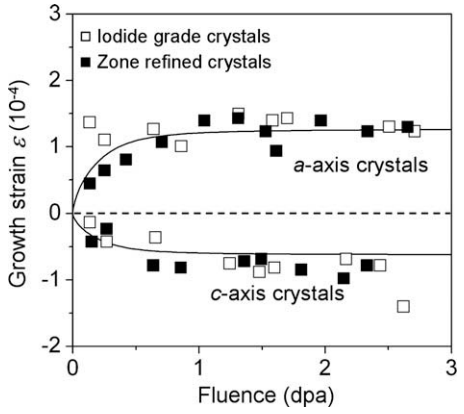

Fig. 2. Irradiation growth of *a*-axis and *c*-axis zirconium single crystals at 553 K. Neutron irradiation (6.5×10^{17} nm^{-2} s^{-1} $\approx 10^{-7}$ dpa s^{-1}). Calculated growth curves compared with experimental points from Rogerson [19].

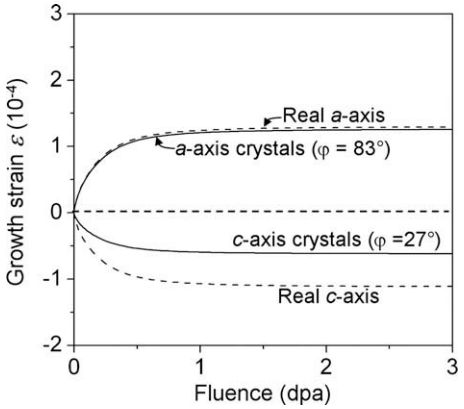

Fig. 3. Comparison between growth along the real crystallographic *a*-axis and *c*-axis (dotted lines) and growth along the main axis of the single crystals (full lines).

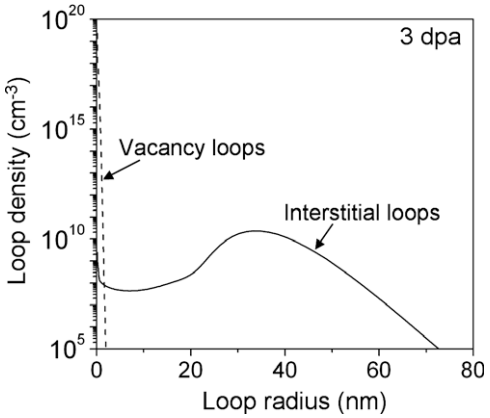

Fig. 4. Vacancy and interstitial prismatic loop size distribution calculated by the Cluster Dynamics Model at a fluence of 3 dpa. The growth of interstitial loops is clearly evidenced.

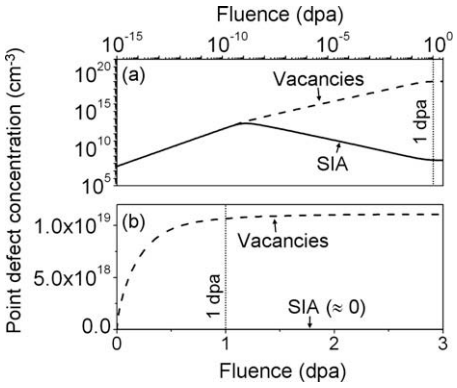

Fig. 5. Variation of point defect concentration during irradiation: (a) conventional logarithmic plot and (b) linear plot. The permanent regime is shown to be reached around 1 dpa.

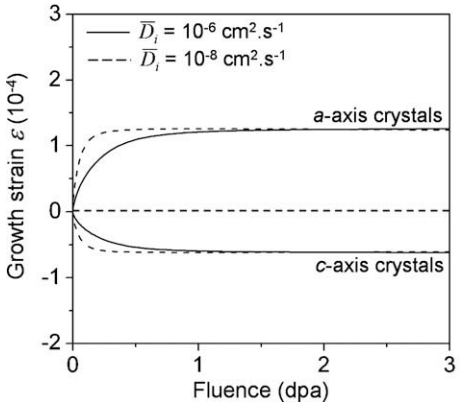

Fig. 7. Influence of the SIA diffusion coefficient $\overline{D}_i$ on the calculated growth curves. Every other input was kept constant (see Table 1).

along the *c*-axis is concerned, we made the assumption that it is due to vacancy relaxation. This contraction is then directly linked to the variation of the vacancy concentration during irradiation. The variation of point defect concentration during irradiation is presented in Fig. 5. The permanent regime is shown to be reached around 1 dpa.

In the calculation shown above, the SIA and vacancy diffusion coefficient $\overline{D}_i$ and D_v were adjusted to get the best fit between the calculated growth curves and the experimental points. We will briefly detail in the following the influence of D_v and $\overline{D}_i$ on the calculated growth curves. Fig. 6 shows the growth curves for two different vacancy diffusion coefficients (every input except vacancy diffusion coefficient was kept constant). It is shown that the strain in the permanent regime increases when the vacancy diffusion coefficient decreases. This can be interpreted by taking into account the influence of the vacancy diffusion coefficient on the vacancy concentration C_{1v} in the permanent regime that is given by Eq. (10) (provided that the dislocation sink strength is low enough) [36–38]:

$$C_{1v} \approx \sqrt{\frac{Gz_i}{4\pi r_{iv} D_v V_{at}}}. \tag{10}$$

From Eqs. (8) and (10), we get:

$$\varepsilon_a \approx \sqrt{\frac{Gz_i V_{at}}{16\pi r_{iv} D_v}}. \tag{11}$$

It can be simply interpreted from Eq. (11) that the strain ε_a in the permanent regime increases when the vacancy diffusion coefficient decreases. The influence of D_v on the strain along the *c*-axis ε_c could be also interpreted in the same way considering Eqs. (6) and (10).

Fig. 7 shows the growth curves for two different SIA diffusion coefficients (every input except SIA diffusion coefficient was kept constant). It is shown that $\overline{D}_i$ has no effect on the strain in the permanent regime, in agreement with Eq. (11). On the other hand, the growth rate increases when $\overline{D}_i$ decreases, which can seem paradoxical. This is due to the fact that a decrease of $\overline{D}_i$ enhances the nucleation of interstitial loops [39]. Fig. 8 shows the size distribution of interstitial loops calculated by the model at a fluence of 0.2 dpa, i.e. before permanent regime is reached, for $\overline{D}_i = 10^{-6}$ cm^2 s^{-1} and $\overline{D}_i = 10^{-8}$ cm^2 s^{-1}. As expected, a decrease of $\overline{D}_i$ leads to a decrease of the loop mean radius, which is due a lower loop growth rate. On the other hand, a decrease of $\overline{D}_i$ leads to a large increase of the loop density. Finally, at a the fluence of 0.2 dpa, the net quantity of SIA included in the prismatic interstitial loops, and hence the growth strain along the *a*-axis, is higher when $\overline{D}_i = 10^{-8}$ cm^2 s^{-1}.

To conclude about the effect of D_v and $\overline{D}_i$ on the strain curves, we can say that D_v affects the level of strain in the permanent regime (above 1 dpa) whereas $\overline{D}_i$ affects the growth rate in the transient regime (below 1 dpa).

We will now compare the values of D_v and $\overline{D}_i$ that we have adjusted in our calculations with the values available in the literature. The SIA diffusion coefficient we used is $\overline{D}_i = 10^{-6}$ cm^2 s^{-1} at 553 K. The $\overline{D}_i$ value at 553 K deduced from the molecular dynamics

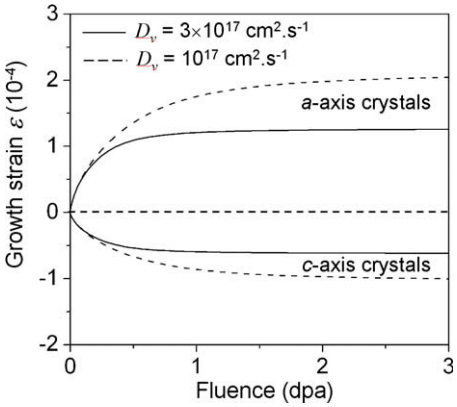

Fig. 6. Influence of the vacancy diffusion coefficient D_v on the calculated growth curves. Every other input was kept constant (see Table 1).

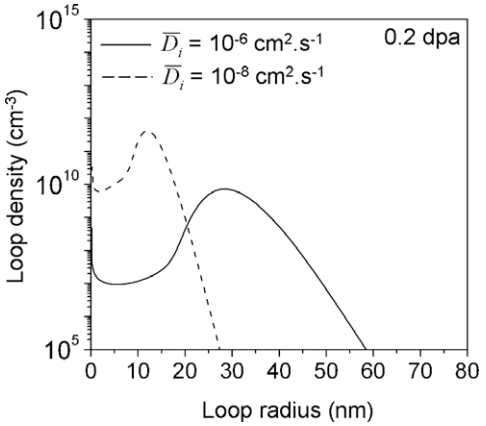

Fig. 8. Influence of the SIA diffusion coefficient $\overline{D}_i$ on the calculated size distribution of prismatic interstitial loops at a fluence of 0.2 dpa.

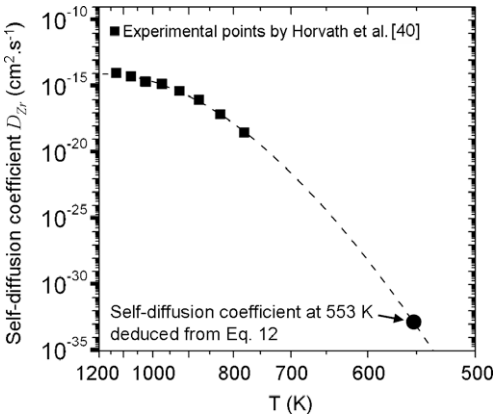

Fig. 9. Arrhenius plot of the self-diffusion coefficient of zirconium. The symbol '•' corresponds to the self-diffusion coefficient estimated from Eq. (12) using $D_v = 3 \times 10^{-17}$ cm^2 s^{-1}.

calculations by Osetsky [11], Woo [12,13] are respectively 5.8×10^{-5}, 1.7×10^{-4} and 8.2×10^{-4} cm^{2}s^{-1}, which is higher than the SIA diffusion coefficient we used. Nevertheless, it must be noticed that the effect of the $\overline{D}_i$ value on the growth curves is not so strong (see Fig. 7) and the growth curves we would obtain with the $\overline{D}_i$ value taken from [11] for example would not fit the experimental points so bad.

The vacancy diffusion coefficient we used is $D_v = 3 \times 10^{-17}$ cm^2 s^{-1} at 553 K. From this D_v value, the zirconium self-diffusion coefficient D_{Zr} can be estimated using Eq. (12):

$$D_{Zr} \approx D_v C_v = D_v \exp\left(-\frac{E_v^f}{kT}\right), \tag{12}$$

where C_v is the equilibrium vacancy concentration at 553 K and E_v^f is the vacancy formation energy ($E_v^f = 1.79$ eV [31]). We get: $D_{Zr} \approx 1.5 \times 10^{-33}$ cm^2 s^{-1}. This value was reported on an Arrhenius plot (Fig. 9) together with the experimental points by Horvath et al. [40]. It is observed that the self-diffusion coefficient estimated from Eq. (12) is in rather good agreement with the experimental points by Horvath et al., provided that we take the downward curvature of the Arrhenius plot into account. We can conclude from this observation that the vacancy diffusion coefficient fitted in the growth calculation ($D_v = 3 \times 10^{-17}$ cm^2 s^{-1}) is not unrealistic. It should nevertheless be recognized that this value is some orders of magnitude below the value proposed by Hood in [41].

3. Cluster Dynamics modelling of zirconium single crystal growth after 'breakaway growth'

The previous section of this paper was devoted to the growth of zirconium single crystals under neutron irradiation for fluences lower than 3 dpa, i.e. before 'breakaway growth' (see Fig. 1). We will now try to model this 'breakaway growth' in order to fit the whole experimental growth curves of Fig. 1.

3.1. Modelling the growth of vacancy loops in the basal planes (c-loops)

From the experimental point of view, it has been demonstrated that breakaway growth corresponds to the formation of *c*-loops lying in the basal planes. They are vacancy in type and their Bürgers vector has a component along the *c*-axis of the lattice structure [26,27]. Moreover, from experimental observation made on zirconium enriched in iron, it has been shown [42] that theses vacancy *c*-loops nucleate on small iron clusters (<1 nm) that lie in the basal planes. Relaxation around these iron clusters lead to Zr_2Fe precipitates [42], the morphology of which is close to a vacancy loop (Fig. 10).

Iron solubility in zirconium is extremely low. Zou et al. [43] proposed an expression of iron solubility in zirconium that is valid between 775 and 970 K. If we extrapolate this expression to 553 K, we find 0.023 at. ppm. Although the single crystals that were used for the growth experiments [18,19] are good purity materials, their iron concentration (54 wt ppm for iodide purity crystals and 10–20 wt ppm for zone refined crystals) are far above the iron solubility.

According to De Carlan [42], these clusters look like small 2-dimensionnal clusters lying in the basal planes (Fig. 10). Their morphology is close to that of vacancy dislocation loops and one can then expect that they could absorb point defects. If the cluster absorbs a net quantity of vacancies, a vacancy loop will nucleate and grow. The iron cluster can then be considered as a vacancy loop nucleation site. On the contrary, concerning absorption of SIA, one can not imagine that an interstitial cluster nucleate on such an iron cluster, taking into account its morphology. This means that the clusters will not be able to absorb SIA unless vacancies have been absorbed first.

In the beginning of irradiation, the sinks usually absorb more SIA than vacancies because $D_i C_{1i} \gg D_v C_{1v}$. In the case of the iron clusters, in the beginning of irradiation, the flux of absorbed SIA will be limited by the flux of absorbed vacancies. In other words, the iron clusters will absorb the same flux of vacancies and SIA.

On the contrary, in the permanent regime ($D_i C_{1i} \approx D_v C_{1v}$), the iron clusters are likely to absorb a little more vacancies than SIA because of SIA diffusion anisotropy. As a consequence, one expects vacancy loops to grow in the basal planes in the permanent regime. This will lead to an unstable situation: indeed, as the basal vacancy loops grow, there sink strength increases and they absorb more and more vacancies, which in turn also means that the prismatic interstitial loops will absorb more and more SIA. One can then understand that the material will grow along the *a*-axis and contract along the *c*-axis faster and faster (breakaway growth). The following of this paper is devoted to the modelling of the breakaway growth by introducing basal loops in the Cluster Dynamics Model.

Some iron clusters were considered in the basal planes that will behave as vacancy loop nucleation sites. Based on the work by De Carlan [42], we will assume that the iron atoms are partially precipitated as small 2-dimensionnal clusters lying in the basal planes (Fig. 10). We will furthermore make the following assumptions:

1. These iron clusters exist before irradiation.
2. The density of iron cluster per unit volume (cm^{-3}) is constant during irradiation.
3. All the iron clusters have a radius of 1 nm.

It will be assumed that, regarding point defect absorption, these iron clusters behave exactly as vacancy *c*-loops (except that their radius cannot be reduced to a value lower than 1 nm by absorption

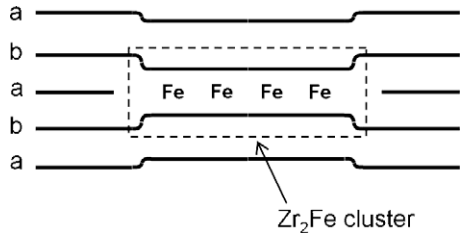

Fig. 10. Morphology of an iron cluster in the basal planes proposed in Ref. [42].

of SIA). The absorption of vacancies and SIA on the *c*-loops is taken into account by adding a term $K_v^c C_{1v}$ and $K_i^c C_{1i}$ to the differential equation describing the variation with time of the vacancy and SIA concentration, respectively. The absorption rates $K_v^c C_{1v}$ and $K_i^c C_{1i}$ ($cm^{-3}\,s^{-1}$) of vacancies and SIA, respectively can be expressed as:

$$\begin{cases} K_v^c C_{1v} = \rho_c Z_v^c D_v C_{1v} \\ K_i^c C_{1i} = \rho_c Z_i^c \overline{D}_i C_{1i} \end{cases}. \tag{13}$$

ρ_c is the *c*-loop line density (cm^{-2}):

$$\rho_c = 2\pi r_c C_c, \tag{14}$$

r_c and C_c are the radius and the density of the *c*-loops per unit volume respectively (it should be noticed that the density C_c of the *c*-loops is equal to that of the iron clusters). The absorption efficiency factor for vacancies is simply:

$$Z_v^c = z_v = 1.0. \tag{15}$$

The absorption efficiency factor for SIA must take into account the SIA / dislocation elastic interaction, but also the SIA diffusion anisotropy (see Ref. [15] for a detailed calculation of Z_i^c as a function of the anisotropy factor p):

$$Z_i^c = z_i p = 1.1 \times p, \tag{16}$$

where p is defined by Eq. (2). Let us define Q_v^c (cm^{-3}) the net number of vacancies absorbed by the *c*-loops. The variation of Q_v^c with time is given by the following differential equation:

$$\frac{dQ_v^c}{dt} = K_v^c C_{1v} - K_i^c C_{1i}. \tag{17}$$

At the beginning of irradiation, $dQ_v^c/dt < 0$ because $\overline{D}_i C_{1i} \gg D_v C_{1v}$ ($C_{1i} \approx C_v$ and $\overline{D}_i \gg D_v$), which would corresponds to the growth of interstitial loops. But, as mentioned above, the nucleation of interstitial loops from the iron clusters lying in the basal planes is not possible, which can be taken into account by considering that $K_i^c C_{1i}$ cannot be higher than $K_v^c C_{1v}$. This means in turn that the *c*-loops can not absorb a given number of SIA unless they have absorbed the same number of vacancies first. The *c*-loops behave in this case as a preferential vacancy/SIA recombination sites, but do not absorb any net flux of point defects.

On the contrary, when the permanent regime is reached, we have $\overline{D}_i C_{1i} \approx D_v C_{1v}$. Nevertheless, because of diffusion anisotropy, $K_v^c C_{1v}$ is slightly higher than $K_i^c C_{1i}$ and then $dQ_v^c/dt > 0$. As a consequence, the *c*-loops will start to grow by absorbing a net number of vacancies, leading to breakaway growth.

In the model, this situation depicted above, in which the *c*-loops will grow or not according to the sign of the term $K_v^c C_{1v} - K_i^c C_{1i}$, can be simply taken into account by rewriting Eq. (17) in the following way:

$$\frac{dQ_v^c}{dt} = \max(0, K_v^c C_{1v} - K_i^c C_{1i}). \tag{18}$$

Assuming that the vacancies agglomerate in a single basal plane, the Bürgers vector of the *c*-loops is $\vec{b} = 1/2\ \langle 0\,0\,0\,1\rangle$ and their radius can be expressed as a function of the net number of absorbed vacancies:

$$r_c = \sqrt{r_{0c}^2 + \frac{Q_v^c S_{at}}{\pi C_c}}, \tag{19}$$

r_{0c} is the initial radius of the vacancy loops (i.e. the radius of the iron clusters on which they nucleate = 1 nm) and S_{at} is the 'area' of a lattice site in the basal plane:

$$S_{at} = \frac{\sqrt{3}}{2} a^2, \tag{20}$$

where a is the lattice parameter of zirconium ($a = 3.23\ 10^{-8}$ cm). The growth curve was calculated using the model until a fluence of 10 dpa for the *a*-axis and the *c*-axis crystals.

It should be emphasized once again that in our model the Fe-rich cluster density is assumed constant over time during irradiation. The possible dissolution and re-precipitation of these clusters due to ballistic mixing by neutron irradiation sometimes discussed in the literature [25,42] was not taken into account here.

3.2. Calculation of the strains along the a-axis, c-axis and crystal axis

The strain along the *a*-axis was calculated the same way as in the previous section (concerning the calculation of growth before breakaway growth) using Eq. (3). The strain along the crystal axis was calculated using Eq. (7). Concerning the strain along the *c*-axis, the contribution of the vacancy *c*-loops was added to Eq. (6):

$$\varepsilon_c = -C_{1v} V_v^{rel} V_{at} - Q_v^c V_{at}. \tag{21}$$

3.3. Results and discussion

The same inputs (Tables 1 and 2) were used as in the previous section. The iron cluster density (cm^{-3}), which also corresponds to the vacancy *c*-loops density (considered constant over time), was adjusted to get the best fit of the experimental points. Fig. 11 shows that the calculated growth curves fit the experimental points very well using a *c*-loops density of $2\ 10^{14}\ cm^{-3}$. It should be emphasized that the general shape of the growth curves and particularly the occurrence of breakaway growth is very satisfactorily modelled.

Considering an iron cluster radius of 1 nm, a volume cluster density of $2\ 10^{14}\ cm^{-3}$ correspond to a molar fraction of precipitated iron of 0.15 ppm. This value is realistic since it is smaller than the total iron molar fraction in the zirconium crystals used for the growth measurements (some tens of wt ppm) [18,19]. It should also be emphasized that the value of the iron cluster radius r_{0c} used in the model has very little influence on the calculated growth curve.

Fig. 12 shows the variation of the loop radius with fluence (interstitial *a*-loops and vacancy *c*-loops). The calculated values of loop radius are close to the experimental measurements available in the literature for the same neutron fluence (some tens of

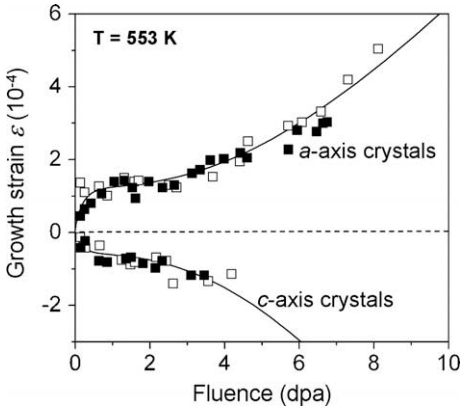

Fig. 11. Irradiation growth of *a*-axis and *c*-axis zirconium single crystals at 553 K. Neutron irradiation ($6.5 \times 10^{17}\ nm^{-2}\ s^{-1} \approx 10^{-7}$ dpa s^{-1}). Calculated growth curves compared with experimental points from Rogerson [18] and Carpenter et al. [19]. The breakaway growth above ~2–3 dpa could be satisfactorily modelled by introducing the growth of vacancy *c*-loops that nucleate on iron clusters lying in the basal planes. A value of $2 \times 10^{14}\ cm^{-3}$ was considered for the density of *c*-loops (i.e. the density of iron clusters).

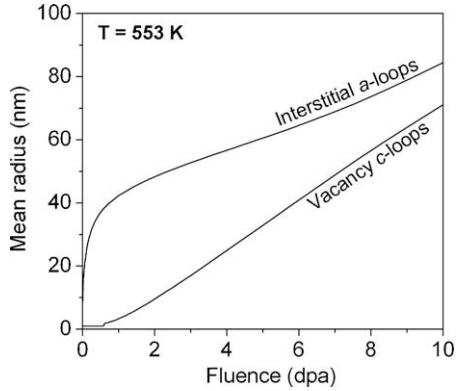

Fig. 12. Calculated variation of the mean radius of the interstitial *a*-loops and the vacancy *c*-loops during irradiation growth.

nm) [22,25,26]. It should be noticed that according to the calculation the vacancy *c*-loops start to grow at a fluence of <1 dpa but their influence on the growth curves start to be really significant only above ~2–3 dpa.

As already mentioned, the value of the iron cluster radius r_{0c} used in the model has very little influence on the calculated growth curve. On the contrary, the value of the iron cluster density per unit volume (that is considered constant over time in the model) strongly affects the calculated growth curves as shown in Fig. 13: the breakaway growth is all the stronger as the iron cluster density in the basal planes is larger. If no cluster iron is considered in the basal planes, no breakaway growth is observed (curve① in Fig. 13). This is easily understandable since the iron clusters act as nucleation sites for the *c*-vacancy loops which are responsible for the breakaway growth.

All the growth curves presented above were calculated at 553 K using a SIA diffusion anisotropy factor of 0.765 [11–13]. The effect of the SIA diffusion anisotropy on the calculated growth curves was checked, considering always the same iron cluster density ($2\ 10^{14}$ cm^{-3}). Fig. 14 shows the calculated growth curves considering two values of the SIA diffusion anisotropy factor ($p = 0.765$ and $p = 1.0$). It is observed that the two curves are rather close to each other for small neutron fluence (<2 dpa). On the contrary, at large fluence, breakaway growth is not observed when SIA diffusion is considered isotropic ($p = 1$), whereas it is observed when $p = 0.765$. This can be interpreted in the following way: it is clear from Eqs. (15) and (16) that, when $p = 1$, Z_v^c is always lower than Z_i^c so that the term dQ_v^c/dt in Eq. (18) can never be positive. The

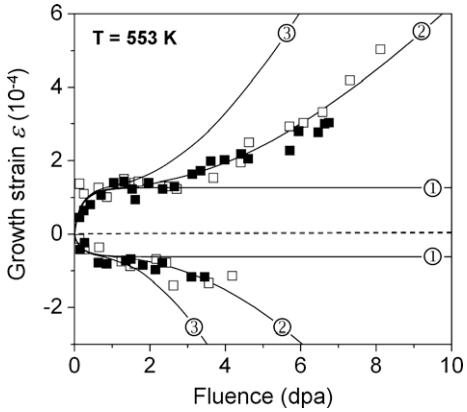

Fig. 13. Influence of the iron cluster density in the basal planes on the calculated growth curves of *a*-axis crystals and *c*-axis crystals. ①: 0, ②: 2×10^{14} cm^{-3}, ③: 10^{15} cm^{-3}. Experimental points from Rogerson [18] and Carpenter et al. [19].

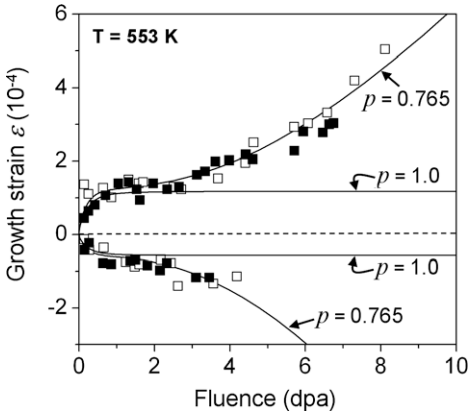

Fig. 14. Influence of the SIA diffusion anisotropy factor *p* on the calculated growth curves of *a*-axis crystals and *c*-axis crystals. $p = 1$ Corresponds to isotropic diffusion of SIA. Experimental points from Rogerson [18] and Carpenter et al. [19].

consequence is that, if $p = 1$, no vacancy loop grow in the basal planes and no breakaway growth is observed.

4. Conclusion

The Cluster Dynamics approach was used in this work to model the irradiation growth of zirconium single crystals as a function of neutron fluence. Taking into account the growth of dislocation loops, as well as the relaxation of vacancies, it was possible to calculate the strain along the two axes of the lattice structure (*a*-axis and *c*-axis), from which the strain was deduced along the main axis of the crystals. The calculation was made as a function of neutron fluence and then compared to the growth measurements by Rogerson [18] and Carpenter et al. [19] on annealed zirconium single crystals at 553 K.

It was shown that the model fits quite nicely the growth measurements made by Rogerson [18] and Carpenter et al. [19], even at large neutron fluence where the 'breakaway growth' is observed. This was made possible by taking into account in the model the growth of vacancy loops in the basal planes. This growth of vacancy loops in the basal planes could be modelled by taking into account that SIA diffusion is anisotropic and that there exist in the basal planes some nucleation sites for vacancy loops (iron clusters), the density of which was considered constant over time.

Appendix. Main features and assumptions of the Cluster Dynamics Model used for the calculation of irradiation growth of zirconium single crystals

Basically the Cluster Dynamics approach is used to describe the variation over time of the size distribution of objects that can grow or shrink according to how they interact with other objects. This technique is very well-adapted to describe agglomeration processes such as solute precipitation or point defect clustering [44,45]. It is based on the general equation:

$$\frac{dC_j}{dt} = G_j + \sum_k w(k,j)C_k - \sum_k w(j,k)C_j - L_j, \qquad (22)$$

where C_j is the concentration of clusters of type *j*, $w(k,j)$ the transition rate per unit concentration of a cluster of type *k* to a cluster of type *j*, G_j the production rate of clusters of type *j* and L_j the loss rate of clusters of type *j* on sinks.

The Cluster Dynamics approach was applied to point defect clustering in [16]. This approach was then extended to materials where point defect diffusion can be anisotropic such as zirconium

[17]. A detailed description of the equations used for the calculation of dislocation loop microstructure variation over time in irradiated zirconium is available in Ref. [17]. We will simply remind here the main features and assumptions of the Cluster Dynamics Model used here for the calculation of zirconium single crystal irradiation growth:

- Only point defects (monomers) are supposed mobile. On the contrary, point defect clusters are assumed immobile.
- SIA diffusion is considered anisotropic (it is considered faster along the *a*-axis than along the *c*-axis). Vacancy diffusion is supposed isotropic.
- Point defect creation, recombination, elimination on dislocation lines and surfaces, and point defect clustering are taken into account.
- It is supposed that only point defects (Frenkel pairs), and not point defect clusters, are created by neutron irradiation.
- The model describes both nucleation and growth of interstitial and vacancy prismatic loops (*a*-loops) with a Bürgers vector $\vec{b} = \frac{1}{3}$ <1 1 2 0>.
- The model describes growth, but not nucleation of basal loops (*c*-loops). Basal loops are assumed to nucleate on pre-existing nucleation sites. These pre-existing nucleation sites are supposed to be Fe-rich clusters, the density of which is assumed to be constant over time. The radius of these Fe-rich clusters is assumed to be 1 nm. The possible dissolution–re-precipitation of Fe-rich clusters during irradiation is not taken into account.
- Deformation is calculated from the total number of point defects absorbed on the dislocation loops. Even small clusters (containing 2 or more point defects) are considered as dislocation loops and are suppose to take part in the deformation.
- Vacancy relaxation is considered anisotropic and is supposed to occur entirely along the *c*-axis. SIA relaxation is neglected.
- Deformation of the zirconium single crystals along the *a*-axis is due to prismatic loops and deformation along the *c*-axis is due to basal loops and vacancy relaxation.

References

[1] J. Nucl. Mater. 159 (1988) 310 – Proceedings of the International Conference on Fundamental Mechanisms of Radiation-Induced Creep and Growth, Hecla Island, Manibota, Canada, 22–25 June 1987.
[2] R. Bullough, M.H. Wood, J. Nucl. Mater. 90 (1980) 1.
[3] E.J. Savino, C.E. Laciana, J. Nucl. Mater. 90 (1980) 89.
[4] S.R. MacEwen, G.J.C. Carpenter, J. Nucl. Mater. 90 (1980) 108.
[5] R.A. Holt, J. Nucl. Mater. 90 (1980) 193.
[6] R.A. Holt, J. Nucl. Mater. 159 (1988) 310.
[7] C.H. Woo, Radiat. Eff. Def. Sol. 144 (1998) 145.
[8] J.R. Fernandez, A.M. Monti, A. Sarce, N. Smetniansky-De Grande, J. Nucl. Mater. 210 (1994) 282.
[9] W. Frank, J. Nucl. Mater. 159 (1988) 122.
[10] D.J. Bacon, J. Nucl. Mater. 159 (1988) 176.
[11] Y.N. Osetsky, D.J. Bacon, N. de Diego, Metall. Mater. Trans. A 33A (2002) 777.
[12] C.H. Woo, H. Huang, W.J. Zhu, Appl. Phys. A 76 (2003) 101.
[13] C.H. Woo, X. Liu, Philos. Mag. 87 (2007) 2355.
[14] C.H. Woo, U. Goesele, J. Nucl. Mater. 119 (1983) 219.
[15] C.H. Woo, J. Nucl. Mater. 159 (1988) 237.
[16] A. Hardouin Duparc, C. Moingeon, N. Smetniansky-de-Grande, A. Barbu, J. Nucl. Mater. 302 (2002) 143.
[17] F. Christien, A. Barbu, J. Nucl. Mater. 346 (2005) 272.
[18] A. Rogerson, R.H. Zee, J. Nucl. Mater. 151 (1987) 81.
[19] G.J.C. Carpenter, R.A. Murgatroyd, A. Rogerson, J.F. Watters, J. Nucl. Mater. 101 (1981) 28.
[20] V. Fidleris, R.P. Tucker, R.B. Adamson, in: R.B. Adamson, L.F.P. van Swam (Eds.), Seventh International Symposium, ASTM STP 939, 1987, p. 49.
[21] C.H. Woo, Neutron-induced displacement damage analysis, Report AECL-6189, Atomic Energy of Canada Limited, 1978.
[22] M. Griffiths, J. Nucl. Mater. 159 (1988) 190.
[23] M. Griffiths, M.H. Loretto, R.E. Smallman, J. Nucl. Mater. 115 (1983) 313.
[24] M. Griffiths, M.H. Loretto, R.E. Smallman, Philos. Mag. A 49 (1984) 613.
[25] M. Griffiths, R.W. Gilbert, J. Nucl. Mater. 150 (1987) 169.
[26] R.A. Holt, R.W. Gilbert, J. Nucl. Mater. 137 (1986) 185.
[27] M. Griffiths, R.A. Holt, A. Rogerson, J. Nucl. Mater. 225 (1995) 245.
[28] O. Le Bacq, F. Willaime, Phys. Rev. B 59 (1999) 8508.
[29] C.K. Ong, Phys. Stat. Sol. B 112 (1982) 321.
[30] P. Ehrhart, K.H. Robrock, H.R. Schober, in: R.A. Johnson, A.N. Orlov (Eds.), Physics of Radiation Effects in Crystals, Elsevier, Amsterdam, 1986, p. 3.
[31] G.J. Ackland, S.J. Wooding, D.J. Bacon, Philos. Mag. A 71 (1995) 553.
[32] R.C. Pasianot, A.M. Monti, J. Nucl. Mater. 264 (1999) 198.
[33] S.R. MacEwen, R.H. Zee, R.C. Birtcher, C. Abromeit, J. Nucl. Mater. 123 (1984) 1036.
[34] P. Ehrhart, B. Schönfeld, in: J.I. Takamura, M. Doyama, M. Kiritani (Eds.), Point Defects and Defect Interactions in Metals, North Holland, Amsterdam, 1982, p. 47.
[35] C.H. Woo, Philos. Mag. 63 (1991) 915.
[36] R. Sizmann, J. Nucl. Mater. 69–70 (1978) 386.
[37] M. Kiritani, H. Takata, J. Nucl. Mater. 69–70 (1978) 277.
[38] F. Christien, A. Barbu, J. Nucl. Mater. 324 (2004) 90.
[39] L.M. Brown, A. Kelly, R.M. Mayer, Philos. Mag. 19 (1969) 721.
[40] J. Horvath, F. Dyment, H. Mehrer, J. Nucl. Mater. 126 (1984) 206.
[41] G.M. Hood, J. Nucl. Mater. 159 (1988) 149.
[42] Y. De Carlan, C. Regnard, M. Griffiths, D. Gilbon, C. Lemaignan, ASTM Special Techn. Pub. 1295 (1996) 638.
[43] H. Zou, G.M. Hood, J.A. Roy, R.J. Schultz, J. Nucl. Mater. 210 (1994) 239.
[44] M.R. Hayns, J. Nucl. Mater. 56 (1975) 267.
[45] L.K. Mansur, J. Nucl. Mater. 216 (1994) 97.